JOURNAL OF COMPUTATIONAL PHYSICS 109, 238–246 (1993)

A New Free Surface Model for the Dip Coating Process

O. RÉGLAT, R. LABRIE, AND P. A. TANGUY*

Department of Chemical Engineering, Université Laval, Québec, Canada G1K 7P4

Received July 15, 1992; revised February 9, 1993

A new iterative finite element solution methodology for free surface flow problems is presented. The approach is based on an explicit projection of the free surface conditions onto a moving boundary, which is iteratively updated using a combination of an adaptive nodal displacement scheme, a B-spline smoothing, and a remeshing of the flow domain. The methodology is tested successfully on the dip coating problem.

INTRODUCTION

The computation of viscous fluid flows with free surface is an important research topic with many applications in material shaping processes (extrusion die swell, mould filling) and coating operations. The dynamics of the free surface is governed by the combination of viscocapillary effects and gravity which makes the simulation particularly awkward, especially in the context of non-Newtonian fluids. At steady state, the equilibrium of the free surface is governed by three conditions, namely: the equality of normal tractions, tangential tractions across the free boundary, and a mass balance across the interface. As the location of the free surface is often unknown, it must be determined simultaneously with the velocity and pressure fields. From a mathematical standpoint, the computation of the free boundary introduces a non-linearity in the equations of change which then must be solved iteratively. Therefore the problem becomes an initial value problem whose convergence depends on the quality of the initial guess as well as the performance of the resolution method.

Finite element simulation of free surface problems has generated a lot of interest for almost 20 years. The first significant contribution used an iterative scheme based on successive substitution [14]. From an initial free boundary shape, the method simulated the flow field using only the first two free surface conditions. The third condition was used to generate a new free surface shape and the procedure was repeated until convergence. An alternate combination was proposed by Orr and Scriven [15], where the free surface was updated with the normal stress equilibrium condition.

The algorithm proposed by Tanner *et al.* [24] which uses the kinematic condition for the update of the free surface position seems to be the most tractable with the finite element method, because the velocity components are obtained directly at the free boundary nodes. However, as pointed out by Silliman and Scriven [19], this choice is suitable only when the viscous effects dominate over the surface tension effects; otherwise the normal stress equilibrium should be preferred. From a practical point of view, the use of the kinematic condition exhibits some drawbacks. The number of iterations to reach convergence can be quite large and depends strongly on the quality of the initial guess. Moreover, when a stagnation point appears on the free boundary, the kinematic condition does not provide an efficient way of updating the free surface in the stagnancy region.

Several nodal displacement schemes for free surface flows are available in the literature, but our experience shows that there is not a unique answer for all problems and that the efficiency of a given algorithm depends on many characteristics such as the shape of the free surface, the existence of stagnation points and/or contact lines, and the quality of the initial guess.

One of the most interesting schemes published so far was proposed by Saito and Scriven [18]. They introduced a new degree of freedom on each free surface node which represents the position of this node. They resolved simultaneously the flow equations and the free surface equation, using a Newton's iteration process. The major advantage of this formulation is that the velocity field and the free surface displacement are computed implicitly, and the free surface does not have to be manipulated. Since the problem is an initial value one, care must be taken in the selection of an appropriate initial guess since the quality of the guess directly influences the convergence properties. Several options to find a successful start-up approximation are available such as experimental evidence, rough physical

* Author for correspondence.

0021-9991/93 $5.00

modelling, or the resolution of an asymptotic approximation of the problem [12].

The purpose of this work is to develop a new formulation for free surface problems which alleviates the difficulty of searching for a good initial free surface guess. The proposed method can be seen as an extension of the original work of Saito and Scriven. It is based on a prediction/projection fixed-point iterative scheme, where the projection step of the free boundary conditions is performed explicitly. A combination of an original nodal displacement scheme, in combination with B-spline smoothing and remeshing, is used for the updating of the free surface. We illustrate the proposed method with the well-known cylindrical dip coating problem.

DIP COATING PROBLEM

We consider the case when a cylindrical substrate is withdrawn vertically at steady state from a fluid-filled reservoir (Fig. 1). This operation known as dip coating is of interest in several manufacturing processes, in particular the food industry. This problem has been the object of several experimental and numerical investigations [21–23, 10], which provide a wealth of data for comparison purposes. In the present study, we will restrict our attention to Newtonian fluids and we will use the set of operating conditions and experimental data published in [21]. The range of flow conditions corresponds to a situation where the surface tension has a moderate to mild influence on the free surface.

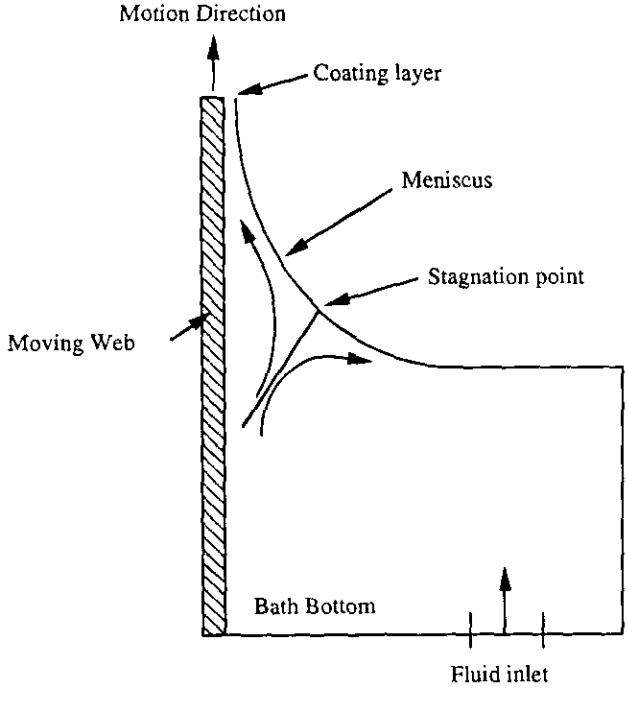

FIG. 1. Dip coating process.

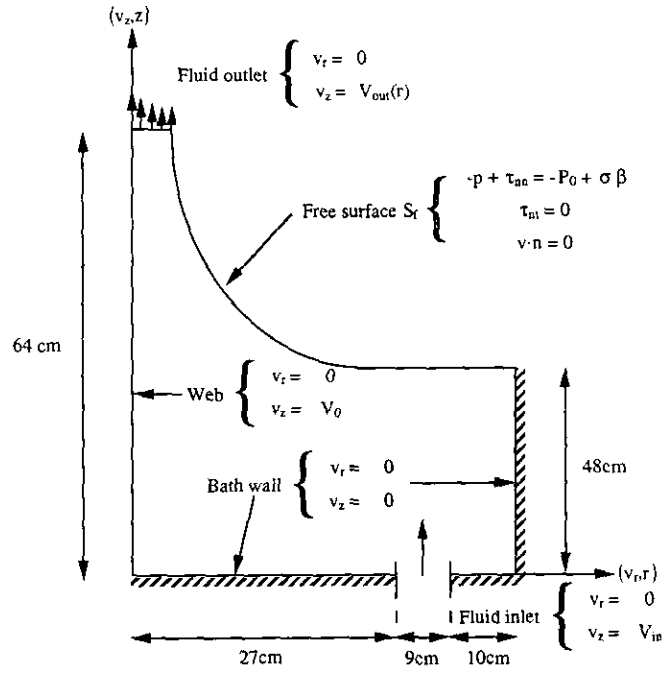

FIG. 2. Boundary condition of the dip coating problem.

The boundary conditions of the problem under consideration are given in Fig. 2. They consist of Dirichlet (velocity) conditions on known boundaries, and mixed Dirichlet–Neumann (velocity–stress) conditions on the free surface S_f. At steady state, the position of the meniscus is governed by:

— the equality of normal stresses across the free boundary;

— the absence of friction (the viscosity of air is assumed to be negligible);

— a no-flow condition across the interface (kinematic condition) which arises from the fact that the free surface is a streamline.

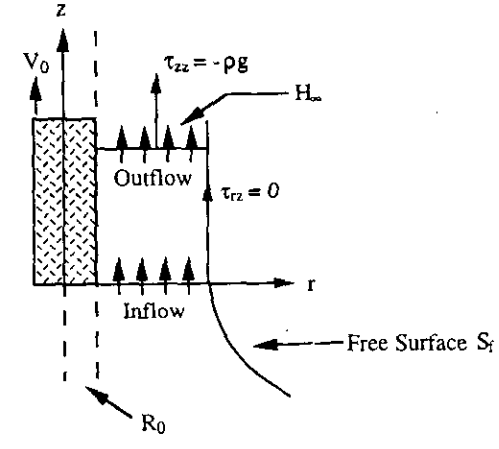

FIG. 3. Boundary conditions at the upper part of the meniscus.

For the outgoing flow and following Tanguy *et al.* [21, 22], a velocity profile is computed assuming a pure shear flow (Fig. 3), which yields

$$V_{\text{out}} = \rho g((r^2 - R_0^2)/2 - H_\infty^2 \log r/R_0)/2\mu + V_0, \quad (1)$$

where R_0 is the radius of the web and H_∞ is the coating thickness far from the meniscus. The inlet flow in the reservoir is adjusted to ensure mass conservation.

GOVERNING EQUATIONS

The partial differential equations governing the conservation of mass and momentum at steady state in the dip coating problem are the classical Navier-Stokes equations:

$$\rho v \cdot \text{grad } v - \text{div } \pi = f, \quad (2)$$

$$\text{div } v = 0, \quad (3)$$

$$\pi = -p\,\delta - \tau, \quad (4)$$

where v is the velocity vector, p is the pressure, ρ is the fluid density, and f is an external force density. The deviatoric tensor τ is expressed by

$$\tau = -2\mu\dot{\gamma}, \quad (5)$$

$$\dot{\gamma} = \tfrac{1}{2}[\nabla v + (\nabla v)^{\mathrm{T}}], \quad (6)$$

where μ is the fluid viscosity.

Considering the curvature of the free boundary, it is convenient to parametrize the boundary by the curvilinear parameter s and introduce a local frame of reference (n, t), where n is the outward oriented normal and t is the tangential vector. In this frame of reference, the stress boundary conditions and the kinematic condition are written

$$-p + \tau_{nn} = -P_0 + \sigma(1/R_1 - 1/R_2) = -p_0 + \sigma\beta \quad (7)$$

$$\tau_{nt} = 0 \quad (8)$$

$$v \cdot n = 0, \quad (9)$$

where τ_{nn} and τ_{nt} are respectively the normal and tangential stress components, P_0 is the atmospheric pressure, σ is the surface tension, R_1 and R_2 are the first and second principal radii of curvature of the free surface S_f, and finally β is the mean curvature of S_f.

Due to the axisymmetric nature of the dip coating problem that we are tackling, the following equivalent definition of β (cf. Keunings [11], for instance) can be conveniently adopted for the algebraic manipulations:

$$\beta n = -(\partial t/\partial s + n/R_2), \quad (10)$$

where R_2 is usually written as

$$1/R_2 = (dz/ds)/rJ, \quad (11)$$

where $J = ((dr/ds)^2 + (dz/ds)^2)^{1/2}$.

The set of boundary conditions (7), (8), and (9) are satisfied only when the boundary S_f is at equilibrium. In order to compute the eventual position of this interface, we propose to devise an algorithm which projects those three conditions on a "moving" free surface, whose location is subsequently updated with the kinematic condition. Before formulating the projection, it is first necessary to explain the motion procedure.

Let us define $e = (e_y, e_z)$ as the unit vector of the displacement of the free surface. This vector can be chosen as the normal to the surface [25], the direction of the velocity across the free surface [7], or it can be oriented along spines [13]. In the present work, we base the displacement procedure on a combination of those vectors (introduced in a later section) so that each free surface node M_0 is moved to a new position M according to the scheme,

$$OM = OM_0 + he \quad (12)$$

which yields for each coordinate:

$$y = y_0 + he_y \quad (13)$$

$$z = z_0 + he_z. \quad (14)$$

The subscript "0" denotes the current free boundary and the variable h represents the length of displacement. This variable will be discretized as a special degree of freedom in the finite element formulation in the spirit of Saito and Scriven [18]. One can remark that the displacement is not purely Lagrangian in the normal direction.

We now introduce the definitions of the normal and tangent vectors of the local frame of reference on the free boundary. We first define the operator $\text{grad}_c = J^{-1}\,\partial/\partial s$ as representing the differential variation along the parametric curve s. On this curve, the normal and tangent vectors are then written as

$$n = (\text{grad}_c\, z)\, y - (\text{grad}_c\, y)\, z \quad (15)$$

$$t = (\text{grad}_c\, y)\, y + (\text{grad}_c\, z)\, z. \quad (16)$$

By substituting Eqs. (13) and (14) in the above definitions, it can be easily shown that

$$n = n_0 - h\,\mathrm{grad}_c\, e^{\perp} - \mathrm{grad}_c(h)\, e^{\perp} \tag{17}$$

$$t = t_0 + h\,\mathrm{grad}_c\, e + \mathrm{grad}_c(h)\, e, \tag{18}$$

where $e^{\perp} = (-e_z, e_y)$ is the vector orthogonal to the vector e and the vectors n_0 and t_0 are the normal and tangential vectors of the current free boundary, respectively.

If we project the free surface conditions (7)–(9) on the moving free surface (Fig. 4), a straightforward substitution of Eqs. (10), (17), and (18) in their expressions yield

$$\begin{aligned}(-p+\tau_{nn})\, n = &-(P_0 + \sigma/R_2)(n_0 - h\,\mathrm{grad}_c\, e^{\perp} \\ &- \mathrm{grad}_c(h)\, e^{\perp}) - \sigma J\,\mathrm{grad}_c(t_0 + h\,\mathrm{grad}_c\, e \\ &+ \mathrm{grad}_c(h)\, e)\end{aligned} \tag{19}$$

$$\tau_{nt} \cdot t = 0 \tag{20}$$

$$v \cdot n_0 - hv \cdot \mathrm{grad}_c\, e^{\perp} - \mathrm{grad}_c(h)\; v \cdot e^{\perp} = 0. \tag{21}$$

Without an *a priori* knowledge of the free surface location, it is clear that the initial free surface guess may be very far from the actual position. In order to make the search procedure converging, it is often required to underrelax the kinematic condition (21) [1], at least during the first iterations. In order to do so, we suggest using the relation (22), instead of imposing directly $v \cdot n = 0$,

$$v \cdot n/|n| = (1-\alpha)\, v \cdot n_0 \qquad \text{with } \alpha \text{ in the range } (0, 1]. \tag{22}$$

Remark 1. To overcome this problem, a new Lagrangian formulation has been published recently [8] based on the use of the characteristics streamline diffusion method [9].

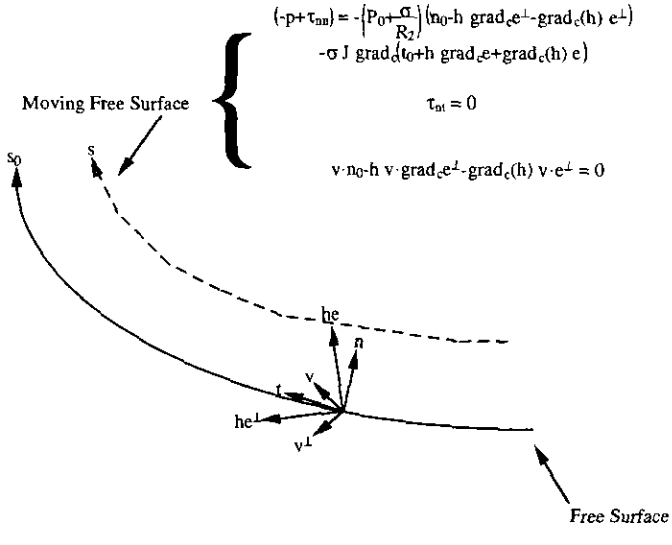

FIG. 4. Projection of the boundary conditions in the moving free surface.

After combining Eqs. (21) and (22), the final form of kinematic condition (used as the updating equation of the free surface) reads

$$\varepsilon v \cdot n_0 - hv \cdot \mathrm{grad}_c\, e^{\perp} - \mathrm{grad}_c(h)\, v \cdot e^{\perp} = 0, \tag{23}$$

where $\varepsilon = (1 - (1-\alpha)\,|n|)$.

FINITE ELEMENT FORMULATION

The equations governing the problem, i.e., Eqs. (2)–(5), (19), (20), and (23) are solved by a Galerkin finite element method. The weak variational form of these equations is

$$a(v, \psi) - b(\psi, p) + c(v, \psi) = (f_1, \psi) + (f_2, \psi) \qquad \forall \psi \in [H_0^1(\Omega)]^3, \tag{24}$$

$$b(v, \Phi) = 0 \qquad \forall \Phi \in L_0^2(\Omega), \tag{25}$$

where

$$a(v, \psi) = \int_{\Omega} \mu \dot{\gamma}(v)\, \dot{\gamma}(\psi)\, d\Omega, \tag{26}$$

$$b(v, \phi) = \int_{\Omega} \phi(\mathrm{div}\, v)\, d\Omega, \tag{27}$$

$$c(v, \psi) = \int_{\Omega} \phi v\, \mathrm{grad}\, v\, d\Omega, \tag{28}$$

$$(f_1, \psi) = \int_{\Gamma} \psi f_1 n\, ds \tag{29}$$

$$(f_2, \psi) = \int_{\Gamma} \psi f_2 t\, ds \tag{30}$$

$$f_1 = -p + \tau_{nn} \tag{31}$$

$$f_2 = \tau_{nt}. \tag{32}$$

The discretisation of the velocity and the pressure is performed with the Crouzeix–Raviart triangular element (enriched quadratic velocity, discontinuous linear pressure) which presents all the necessary conditions of numerical stability and convergence [3].

On the free boundary, the flux terms (31) and (32), after substitution in Eqs. (19) and (20) and integration by parts, become

$$\begin{aligned}F_1(h) = &\int_{\Gamma} \psi(-P_0 - \sigma/R_2)(n_0 - h\,\mathrm{grad}_c\, e^{\perp} \\ &- \mathrm{grad}_c(h)\, e^{\perp})\, ds + \sigma \int_{\Gamma} \partial\psi/\partial s \\ &\times (t_0 + h\,\mathrm{grad}_c\, e + \mathrm{grad}_c(h)\, e)\, ds \\ &- \sigma(\psi_e t_e - \psi_b t_b)\end{aligned} \tag{33}$$

$$F_2(h) = 0, \tag{34}$$

where the subscripts "e" and "b" represent the end-nodes of the free boundary.

In a similar fashion, we can write the weak form of the updating equation (23) as

$$\int_\Gamma \psi(\varepsilon v \cdot n_0 - hv \cdot \operatorname{grad}_c e^\perp - \operatorname{grad}_c(h)\, v \cdot e^\perp)\, ds = 0. \quad (35)$$

An approximation basis must be introduced for h. In our case, we use a standard quadratic Lagrange polynomial, namely,

$$h = \sum_j c_j h_j, \quad (36)$$

where the parameters c_j are the coefficients of the approximation basis. Therefore, it is possible to write Eq. (35) as

$$\sum_j \int_\Gamma \psi(c_j v \cdot \operatorname{grad}_c(e^\perp) + \operatorname{grad}_c(c_j)\, v \cdot e^\perp\, ds\, h_j = \int_\Gamma \psi(\varepsilon v \cdot n_0)\, ds. \quad (37)$$

As for the resolution, we use the classical Uzawa algorithm [6] which allows us to impose as exactly as desired, the incompressibility constraint. The Uzawa algorithm is adapted to symmetric problems. To use it in the context of the Navier–Stokes equations, the nonlinear term is placed in the right-hand side of the equation and iterated upon. It will converge easily for low velocity, high viscosity problems (creeping flows), which is the range of problems that we are dealing with.

The proposed algorithm reads as follows ($1/\varepsilon_p$ is the penalty parameter):

(1) h^n, v^n, and p^n known (start with $v^0 = 0$ and $p^0 = 0$), compute v^{n+1} by solving

$$\mu \operatorname{div}(\operatorname{grad})\, v^{n+1} + 1/\varepsilon_p \cdot \operatorname{grad}(\operatorname{div} v^{n+1}) = \rho f - \operatorname{grad} p^n + v^n \cdot \operatorname{grad} v^n + F_1(h^n).$$

(2) Update p^{n+1} using $p^{n+1} = p^n + 1/\varepsilon_p \cdot \operatorname{div} v^{n+1}$.

(3) Update h^{n+1} by solving Problem 37.

FREE SURFACE UPDATING PROCEDURE

The free surface updating is based on an adaptive nodal displacement procedure, combined with a smoothing of the free boundary and remeshing of the flow domain. For the displacement scheme, i.e., the selection of the unit displacement vector e and $e^\perp$, we suggest using

$$e = c_1 n + c_2 v/|v| \quad (38)$$

$$e^\perp = c_1 t + c_2 v^\perp/|v|, \quad (39)$$

where the coefficients c_1 and c_2 are adaptive control parameters. Depending on the value of these coefficients, it is possible to emphasize a displacement in the normal direction or in the velocity direction. In the former case, the free boundary motion is governed by a pressure force, whereas in the latter one, the motion is driven by a dynamic force.

In order to detect the actual the influence of the parameters, Eqs. (23), (38), and (39) can be combined, which yields

$$(\varepsilon + hc_1/JR_1)\, v \cdot n_0 - hc_2 v \cdot \operatorname{grad}_c(v^\perp/|v|) - \operatorname{grad}_c(h)\, c_1 v \cdot t_0 = 0. \quad (40)$$

We then integrate this equation for the two limiting cases: $c_1 = 1$, $c_2 = 0$ and $c_1 = 0$, $c_2 = 1$, which gives:

Limiting case $c_1 = 1$ *and* $c_2 = 0$,

$$h \approx h_1 + \varepsilon v_n/v_t(1 + h_1/JR_1\varepsilon)\cdot \quad (41)$$

Limiting case $c_1 = 0$ *and* $c_2 = 1$,

$$h = \varepsilon v_n\, |v|/(v \cdot \operatorname{grad}_c v^\perp), \quad (42)$$

where h_1 is the (known) value of h at $s = s_1$, v_n and v_t are the normal and tangential components of the velocity, and $v^\perp$ the vector orthogonal to v.

Remark 2. When $1/R_1 = 0$, Eq. (41) is nothing but the equation of a streamline, and the schemes becomes formally equivalent to the one introduced by Zienkiewics and Godbole [25].

Remark 3. Equation (42) enables us to dampen the large variations of h that sometimes occur when the tangential component of the velocity is very small.

From a practical standpoint, the use of Eq. (12) node by node allows to define a new series of nodes M_i representing the updated free surface. The direct use of these points for the next iteration is, however, not recommended due to the non-uniformity of the free surface shape which can make the iterative process diverging. Rather, we suggest smoothing the new boundary using a B-spline representation [17] of the free surface curve for which each point M_i exerts a local influence. We recall here that a B-spline curve is defined as a series of segments, each of which being represented by K points M_i, where K is the order of the curve. Since one

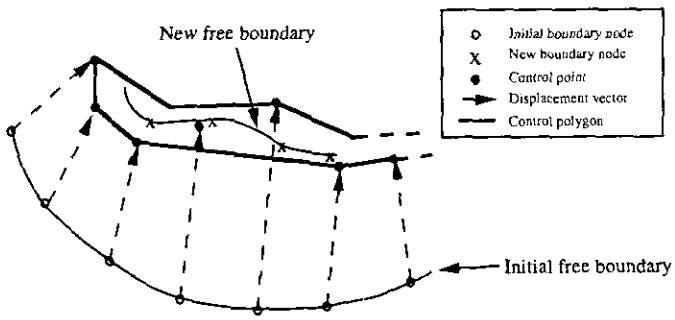

FIG. 5. Free surface updating process.

important property of B-spline curves is that for a cubic B-spline curve, the curvature is continuous, we use $K = 4$ in the present work. This is a property of a streamline, and consequently that of a free boundary.

We show in Fig. 5 the principle of the free surface updating process. The resulting boundary is defined parametrically, which enables us to keep the control on the location of each node and then to ensure that all the elements have roughly the same size. Once the new free boundary is created, the next step is to remesh the whole domain. As we do not use quadrilateral elements, there is no special rule of element orthogonality to satisfy like that in Christodoulou and Scriven [2]. We rather use the low cost, unstructured mesh generator described in Dannelongue and Tanguy [4]. This mesh generator, based on a segment tree data structure (multi-dimensional binary tree), allows us to build elements in a domain and interpolate between meshes at a cost which varies linearly with the number of elements. It also enables us to optimally control the mean size of the elements, an important feature in the context of meniscus flows. This generator was proven to be very superior to more conventional algorithms in the context of adaptive flow problems [5]. Let us finally remark that the use of triangular elements also provides maximum flexibility to mesh topology with a large aspect ratio, as in the dip coating problem.

The free surface algorithm, which comprises the flow computation, the free surface updating, and the B-spline smoothing/remeshing process, is applied iteratively until convergence. To assess the convergence, we introduce a dimensionless parameter called the proximity parameter, namely,

$$P = V_s / V_0, \tag{43}$$

where V_s, a characteristic velocity of the free surface, is defined as

$$V_s = (\Sigma_{nel} \mathbf{v}_n l \cdot r)/(\Sigma_{nel} l \cdot r). \tag{44}$$

In these relations, V_0 is the withdrawal velocity, $\mathbf{v}_n$ is the normal component of the average velocity on a free boundary element edge, l is the length of the element edge, and r is the average radius between the edge and the web (Fig. 6). This definition of the proximity parameter is well adapted to the dip coating problem and it can be seen as the degree of departure between the current solution and the final solution. The free boundary is considered as converged when the proximity parameter P is smaller than a prescribed tolerance.

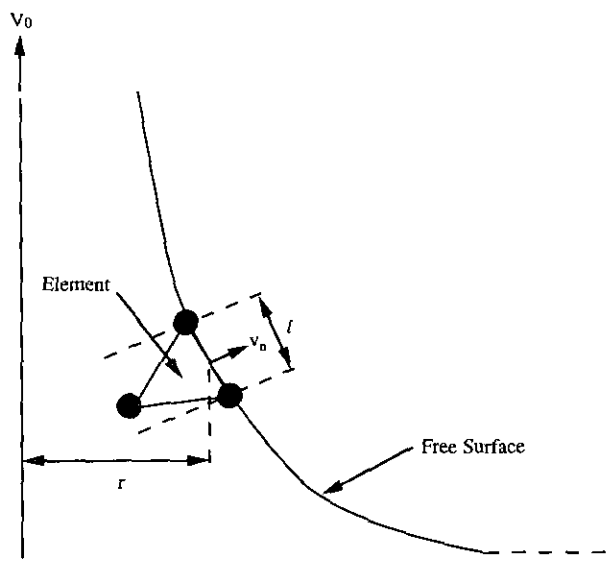

FIG. 6. Notation for the proximity parameter.

APPLICATION

One important feature of this paper is that the proposed free surface algorithm does not require a good initial start-up approximation to converge. In the problem considered, the initial free surface was defined by four horizontal control points and four vertical ones (Fig. 7), which were positioned so that the resulting curve lay inside the final domain. The mesh used at the first iteration (Fig. 7) included 751 elements and 1638 nodes.

The parameters used in the simulation are

$R_0 = 0{,}19$ mm
$V_0 = 2{,}41$ cm/s
$\mu = 2.9$ Pa-s
$\rho = 910$ kg/m^3
$\sigma = 0{,}0359$ N/m.

We show in Fig. 8 the position of the free boundary at the first iteration. It can be seen that this solution is far from the equilibrium because the velocity vectors at the interface have a large magnitude and are almost perpendicular to the boundary. During the subsequent iterations, it was

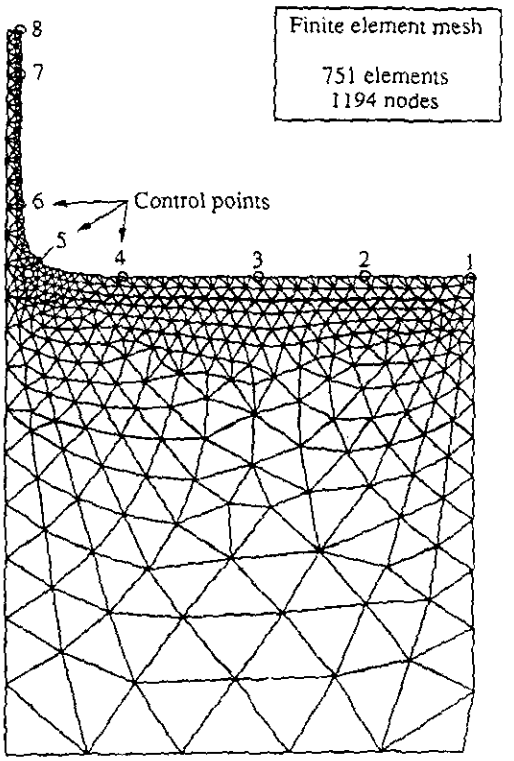

FIG. 7. Free surface control points and finite element mesh at the first iteration.

observed that the free surface behavior was varying, depending on the location on the meniscus. In the horizontal part of the meniscus, the magnitude of velocities is small, and the surface shape becomes rapidly stable. On the other hand, in the upper part of the meniscus, the velocities tend to remain parallel to the meniscus and the eventual coating thickness is obtained much more slowly. This can be partly explained by the dependence of the free boundary motion with respect to the ratio v_n/v_t, i.e., the angle of the velocity vector with the tangent to the surface. During the first iterations, this angle is more pronounced in the horizontal part of the meniscus. Moreover, the height of the reservoir level is not critical for the coating thickness, which means that on the overall, the geometrical constraints are not that important in this region, hence a faster convergence. The final result is shown in Fig. 9, where the location of the stagnation point can be easily noticed.

Remark 4. It should be recalled that a value for the under-relaxation parameter in the updating equation (23) must be selected for practical computations. There is no technique available so far to find an optimal value for α. Numerical tests showed that $\alpha = 0{,}5$ is a suitable choice for the first few iterations; this value can be progressively increased while the procedure converges.

A series of simulations were carried out to assess the role of the control parameters c_1 and c_2 on the convergence

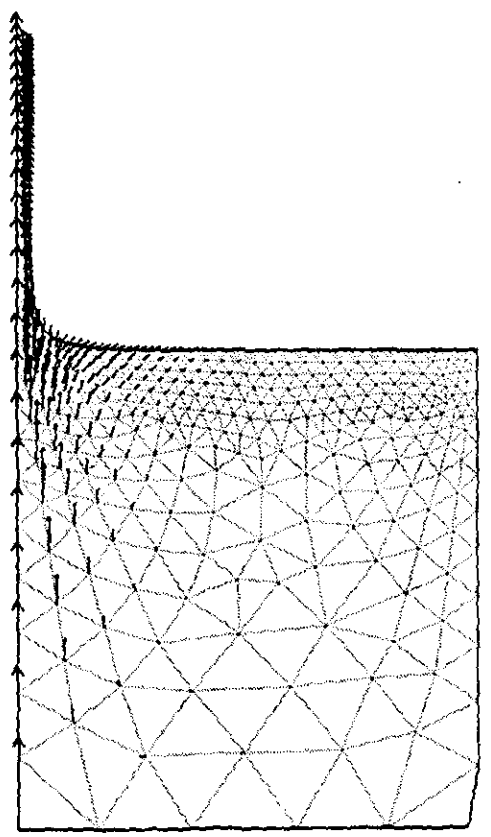

FIG. 8. Flow results (velocity vectors) after the first iteration.

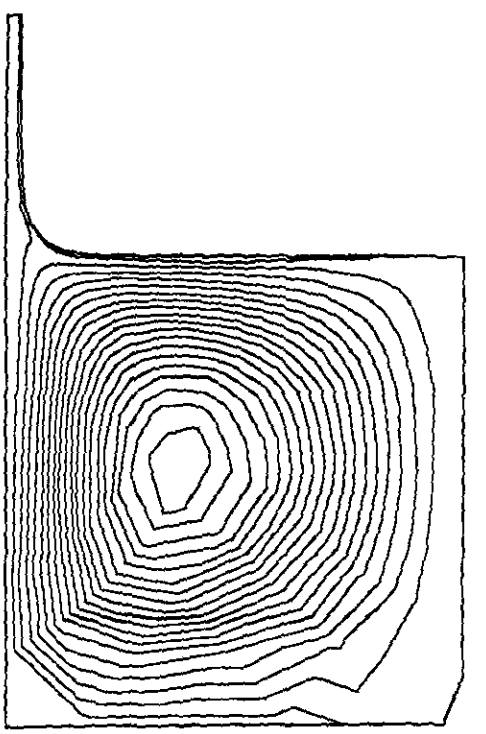

FIG. 9. Streamline pattern and meniscus shape for $V_0 = 2{,}41$ cm/s.

behaviour. Results are presented in Figs. 10a and b in terms of the eventual coating thickness and the proximity parameter P (Eq. (38)) versus the number of iterations. For $c_1 = 0{,}5$ and $c_2 = 1{,}5$, nodal displacement is emphasized in the velocity direction. It can be noted that we obtain a very good accuracy ($P < 5 \times 10^{-3}$), but that the error on the coating thickness is still around 1% after 40 iterations (the "reference" measured value is 1.54 mm). The number of iterations to reach the convergence may appear large, but it is related to the "poor" quality of the initial guess used as the start-up approximation. A better guess would have drastically reduced this number. For $c_1 = 1{,}5$ and $c_2 = 0{,}5$, the nodal displacement in the normal direction is enhanced. The accuracy on P is not as good as in the previous case ($P \approx 7{,}5 \times 10^{-3}$) but the correct value of H_∞ is obtained

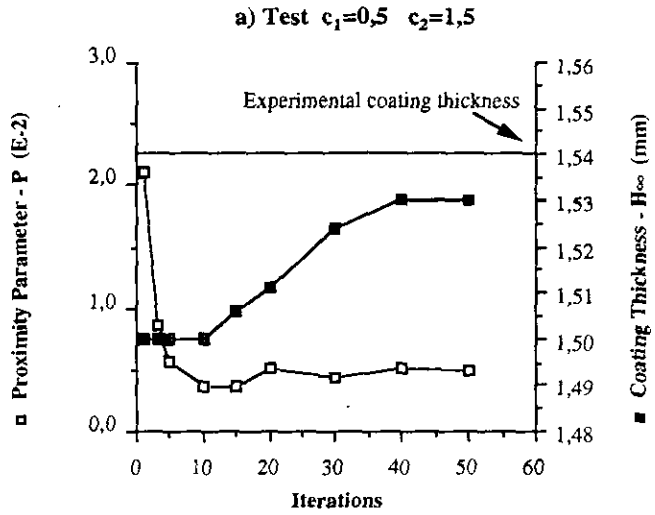

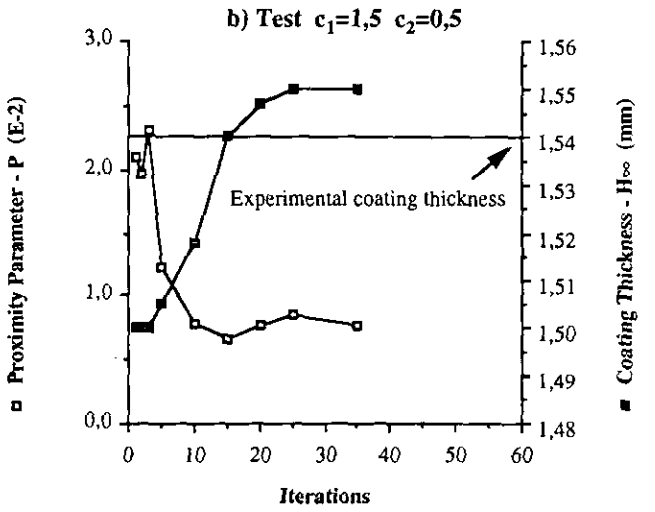

FIG. 10. Convergence history of the free surface: (a) $c_1 = 0{,}5$ and $c_2 = 1{,}5$; (b) $c_1 = 1{,}5$ and $c_2 = 0{,}5$.

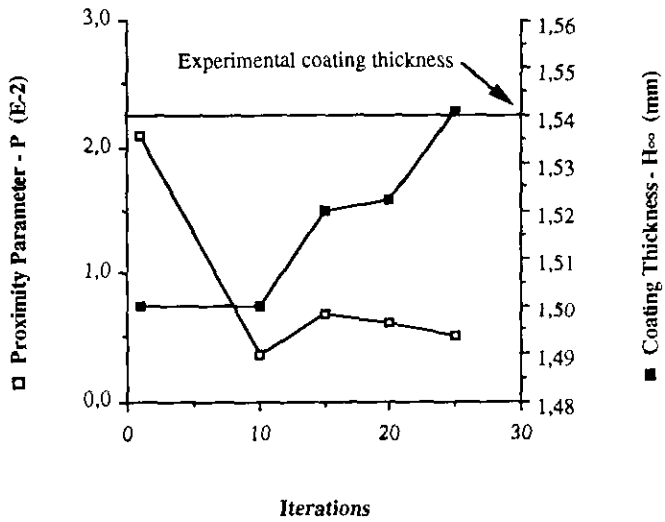

Iterations	c_1	c_2
1	0,5	1,5
10	0,5	1,5
15	1,5	0,5
20	0,3	1,7
25	1,7	0,3

FIG. 11. Convergence history for the free surface with adaptive values for c_1 and c_2.

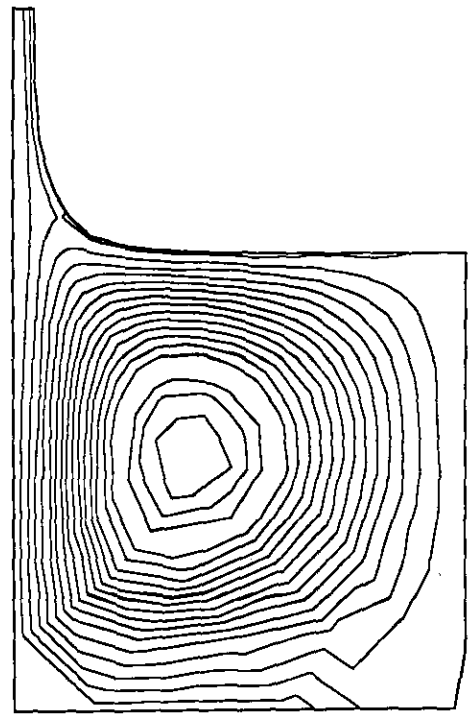

FIG. 12. Streamline pattern and meniscus shape for $V_0 = 7{,}47$ cm/s.

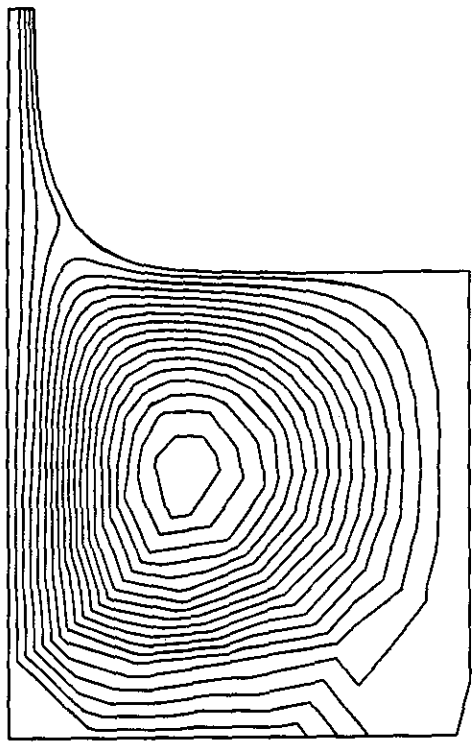

FIG. 13. Streamline pattern and meniscus shape for $V_0 = 12$ cm/s.

after 25 iterations. These two results show that the first scheme is accurate but the second one is fast. In order to combine the advantages of the two schemes, it is required to modify the values of the control parameters during the iteration procedure. We show in Fig. 11 a possible strategy. In the present state of the method, there is no method to select the values and an heuristic approach must be used, based on the convergence trends of the free surface.

We show in Figs. 12 and 13 two additional results obtained with larger withdrawal velocities, $V_0 = 7{,}47$ cm/s and $V_0 = 12$ cm/s, respectively. The streamline patterns show clearly that the eventual meniscus is at equilibrium for the two cases. In terms of coating thickness, a very good agreement is also obtained between the numerical predictions and the experimental data. The reader is referred to Réglat [16] for a more detailed description of these tests.

CONCLUDING REMARKS

We have shown in this work it is possible to compute with very good accuracy the location of the free surface in the dip coating process, starting with an initial guess that is far from the eventual solution. This was made possibly by using a new formulation for the free surface updating procedure based on an iterative projection of the three boundary conditions governing the equilibrium of the free boundary onto a virtual boundary; a B-spline smoothing of the updated interface combined with a remeshing of the flow domain with a low-cost mesh generator was performed at each iteration to avoid oscillations. The method will be tested on new free surface problems to assess the robustness properties as well as to devise a way to choose the control parameters, especially in the case where the surface tension effects strongly influence the equilibrium of the free surface.

REFERENCES

1. B. Caswell and M. Viriyayuthakorn, *J. Non-Newtonian Fluid Mech.* **12**, 13 (1983).
2. K. N. Christodoulou and L. E. Scriven, *J. Comput. Phys.* **99**, 39 (1992).
3. M. Crouzeix and P. A. Raviart, *RAIRO an. num.* **7**, 33 (1973).
4. H. Dannelongue and P. A. Tanguy, *J. Comput. Phys.* **91**, 94 (1990a).
5. H. Dannelongue and P. A. Tanguy, *Int. J. Numer. Methods Eng.* **30**, 1555 (1990b).
6. M. Fortin and R. Glowinski, *Augmented Lagrangian Methods* (North Holland, Amsterdam, 1983).
7. C. S. Frederiksen and A. M. Watts, *J. Comput. Phys.* **39**, 282 (1981).
8. P. Hansbo, *Comput. Methods Appl. Mech. Eng.* **99**, 171 (1992).
9. P. Hansbo, *Comput. Methods Appl. Mech. Eng.* **96**, 239 (1992).
10. P. Hurez and P. A. Tanguy, *Polym. Eng. Sci.* **30**, 1125 (1990).
11. R. Keunings, *J. Comput. Phys.* **62**, 199 (1986).
12. S. F. Kistler, Ph.D. thesis, University of Minnesota, 1984.
13. S. F. Kistler and L. E. Scriven, *Int. J. Numer. Methods Fluids* **4**, 207 (1984).
14. R. E. Nickell, R. I. Tanner, and B. Caswell, *J. Fl. Mech.* **65**, 189 (1974).
15. F. M. Orr and L. E. Scriven, *J. Fluid Mech.* **84**, 145 (1978).
16. O. Réglat, M. Sc. thesis, Laval University, 1991.
17. D. F. Roger and J. A. Adams, *Mathematical Elements for Computer Graphics* (McGraw-Hill, New York, 1990).
18. H. Saito and L. E. Scriven, *J. Comput. Phys.* **42**, 53 (1981).
19. W. J. Silliman and L. E. Scriven, *J. Comput. Phys.* **34**, 287 (1980).
20. P. Tanguy, Ph.D. thesis, Laval University, 1982.
21. P. Tanguy, M. Fortin, and L. Choplin, *Int. J. Numer. Methods Fluids* **4**, 445 (1984).
22. P. Tanguy, M. Fortin, and L. Choplin, *Int. J. Numer. Methods Fluids* **4**, 457 (1984).
23. P. Tanguy, L. Choplin, and M. Fortin, *Can J. Chem. Eng.* **63**, 533 (1985).
24. R. I. Tanner, R. E. Nickell, and R. W. Bilger, *Comput. Methods Appl. Mech. Eng.* **6**, 155 (1975).
25. O. C. Zienkiewicz and P. N. Godbole, *Finite Element in Fluids*, edited by R. H. Gallager (Wiley, New York, 1975), Vol. 1, p. 25.